HEAT STRESS MODELING USING NEURAL NETWORKS TECHNIQUE

Aiman Mazhar Qureshi, Ahmed Rachid

Available online at www.sciencedirect.com

ScienceDirect

IFAC PapersOnLine 55-12 (2022) 13–18

HEAT STRESS MODELING USING NEURAL NETWORKS TECHNIQUE

Aiman Mazhar Qureshi*, Ahmed Rachid**

** University of Picardie Jules Verne, Amiens, CO 80000 France (corresponding author, phone: +33601535460; email: aiman.mazhar.qureshi@etud.u-picardie.fr)*

*** University of Picardie Jules Verne, Amiens, CO 80000 France. (e-mail: ahmed.rachid@u-picardie.fr)*

Abstract: Rising temperature especially in summer is currently a hot debate. Scientists around the world have raised concerns about Heat Stress Assessment (HSA). It depends on the urban geometry, building materials, greenery, environmental factor of the region, psychological and behavioral factors of the inhabitants. Effective and accurate heat stress forecasts are useful for managing thermal comfort in the area. A widely used technique is artificial intelligence (AI), especially neural networks, which can be trained on weather variables. In this study, the five most important meteorological parameters such as air temperature, global radiation, relative humidity, surface temperature and wind speed are considered for HSA. System dynamic approach and a new version of the Gated Recurrent Unit (GRU) method is used for the prediction of the mean radiant temperature, the mean predicted vote and the physiological equivalent temperature. GRU is a promising technology, the results with higher accuracy are obtained from this algorithm. The results obtained from the model are validated with the output of reference software named Rayman. Django's graphical user interface was created which allows users to select the range of thermal comfort scales based on their perception which depends on the age factor, local weather adaptability, and habit of tolerating the heat events. It also gives a warning to the user by color code about the level of discomfort which helps them to schedule and manage their outdoor activities. Future work consists of coupling this model with urban greenery factors to analyze the impact on the estimation of heat stress.

Keywords: Artificial intelligence, thermal comfort, modeling, system dynamic approach and urban heat stress.

1. INTRODUCTION

In 2003, Europe experienced the driest and hottest summer since AD 1500, responsible for the death toll of 30,000 from the heat. Encountering this, team of scientists (Poumadere et al., 2005) suggested that this European heat wave could have occurred due to climate change. The increase in temperature worsens health problems. In addition, from a physiological point of view, during peak summers, when the temperature exceeds the normal tolerance limit of the human body which can lead to circulatory collapse or dehydration leading to death. It becomes unfavorable in a vulnerable population, comprising of children, old aged people, and handy-capped people (Luber and McGeehin, 2008).

Due to human activities, the properties of the local climate are altered (Kalnay and Cai, 2003). Urbanization around the world is happening at an accelerating rate, with global warming which is increasing Heat Stress (HS). It is imperative to identify certain factors that contribute to the intensification of HS (Fischer and Schär, 2010),(McDonald et al., 2011). In general, the external factors that influence the formation of Urban Heat Stress (UHS) are: seasons, synoptic conditions and climate. There are many researchers have worked hard to extract the influence of meteorological parameters on HS (Arnds et al., 2017, Hoffmann, 2012, Hoffmann and Schlünzen, 2013 b, Ivajnšič and Žiberna, 2019).

Many parameters are considered while calculating HS in metropolitan cities (Akbari et al., 1990). The fundamentals of various numerical micro-scale models emphasize the synergy of urban fabric (land surface and building materials) and meteorological parameters; solar radiation (diffuse, direct), airflow and heat transfer from open surfaces (Grimmond, 2007). Air temperature (T_{air},) is the most used input parameter, followed by mean radiant temperature (T_{mrt}), after surface temperature (T_s) has been applied, and rarely wind speed (W_s) was used as an input parameter (Mirzaei, 2015). In 2019, a study on assessment of thermal comfort in open urban areas used the input factors; location, activity, gender, locality, age group, temperature of the globe, T_{air} , Solar Radiation (SR), Relative Humidity (RH), W_s, wind direction and the output was Predicted Mean Vote (PMV), Physiological Equivalent Temperature (PET), T_{mrt} and Standard Effective Temperature (SET) (Tsoka et al., 2018). In another study, an advanced algorithm based on neuro-fuzzy logic was attempted to create predictive models (Kicovic et al., 2019) and concluded that SR has the highest impact compared to T_{air} on thermal comfort of visitors in urban areas. In 2019, team of Kuala Lumpur University Campus worked on the Heat Stress Assessment (HSA). The

10.1016/j.ifacol.2022.07.281

following meteorological data was used in their research as input variables: W_s, wind direction, initial atmospheric temperature, RH, cloud cover, location, soil data, building characteristics, walking speed, mechanical factor, heat transfer, clothing data to calculate T_{mrt}, PMV and PET values. T_{mrt} is the key meteorological parameter that affects the human energy balance, PMV and PET are significant indices, which are under the influence of T_{mrt} (Ghaffarianhoseini et al., 2019). In Previous studies urban geometry with green adaptive measures were missing during estimation of HS which is extremely difficult, mainly due to the complexity of the urban system. Artificial intelligence (AI) is a widely used technique to deal such problems. The support vector machine (SVM) is machine learning approach was used for the estimation of PMV. The results obtained with 76.7% accuracy which was twice as high as the widely adopted Fanger model which has an accuracy of 35% (Farhan et al., 2015). Recently, deep learning (DL) approaches have been reported with high precision results. Particularly, Convolutional and Long-Short Term Memory (LSTM). Recurrent Neural Networks (RNNs) have been used to predict hourly T_{air} with much less error (Hewage et al., 2021). In this study, a system dynamic approach is used for choosing the influenced variables of weather for HSA. The Rayman model (Matzarakis et al., 2007b, Matzarakis et al., 2010) is initially used for collection of simulated PET, PMV and T_{mrt} data and for comparative reference.

The recurrent neural network (RNN) with memory function is used for modeling which is apparently more suited to this type of task. In this article, we make 3 contributions.

- We used Gated Recurrent Units (GRU) networks (Cho et al., 2014), which largely contributes to mitigating the problem of gradient vanishing of RNNs through the gating mechanism and simplify the structure while maintaining the effect of LSTM.
- High precision is achieved by the model and coupled with a friendly user interface that recognizes the individual thermal sensation level corresponding to the results.
- The database makes it possible to analyze the thermal comfort scales chosen by the users.
- The developed model is flexible, which will allow in the future to couple it with real data on the cooling effect of urban greenery and estimate the absolute HS for individuals.

The remainder of this paper is organized as follows: the methodology is discussed in section 2, section 3 covers the model framework and experimental results. Section 4 presents framework of the GUI. Finally, conclusion in section 5.

2. METHODOLOGY

2.1 Systemic Dynamic Approach

As mentioned in the previous section that the mitigation of thermal discomfort caused by climate change is todays challenge; it happens due to a complex environment where multiple parameters are involved with their known behavioral feedback. To encounter this complex issue, a holistic dynamic systems approach is used which connects and emerge various influencing variables and address the nonlinear and linear interactions between them. This article proposes a systems dynamic modeling approach to simulate HS in a complex environment using interdependent factors that are strongly influenced by UHS. The systematic approach of this study is presented in Fig.1.

Most often, there is an uncertainty about the responses and strengths of interactions in such model, but it is always contented to see conditions resulting in behaviors that are plausible and internally consistent. The systems approach allows user to compare a number of assumptions and alternative strategies and it makes the model simple to understand, without trivializing the underlying assumptions and interrelated processes.

Fig.1 System dynamic approach for the assessment of heat stress

2.2 Data Generation

The Rayman model is beneficial for wave radiation flux densities in complex or simpler environments (Matzarakis et al., 2007 b). It is used throughout the simulation for data generation. Four variables such as GR, RH, T_{air} and W_s were considered as the main input variables for the calculation of PMV, PET and T_{mrt}. The calculated strategy consisted of varying a one variable for each simulation and it was repeated for every point to observe the variations of each input on the output.

2.3 Data Selection

The output data file is received with T_{mrt}, PMV, PET, thermal radiation (TR) and T_s corresponding to the main input variables. Later, the data was further analyzed by correlation coefficient against each output variable and evaluated the significant influential input variable affecting the behavior of the system Fig.2 shows the correlation of the most influenced input variables affecting the output variables (i.e., PMV, PET, T_{mrt}). We included 5 important variables as inputs (X) with 3 outputs (Y) while the remaining variables found with low dependence were neglected.

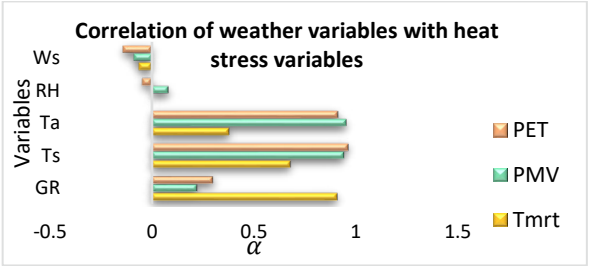

Fig.2 Correlation of weather variables with heat stress

3. MODELING FRAMEWORK

The final and stabilized model was produced in several stages. The frame work is shown in Fig.3 and each procedure

is discussed in the following subsections.

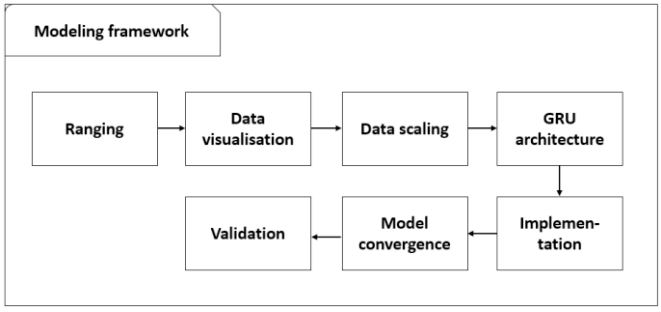

Fig.3 Modeling Framework

3.1 Data Ranging

Data ranging helps to determine the number of different classes present in the data and gives the basic idea of the certainty of output below the range of input limits. It also helps to understand the distribution and spreading range of the data by looking at the mean value, the standard deviation and percentile distribution for numeric values. Graphical presentation of the data ranging is shown in Fig.4.

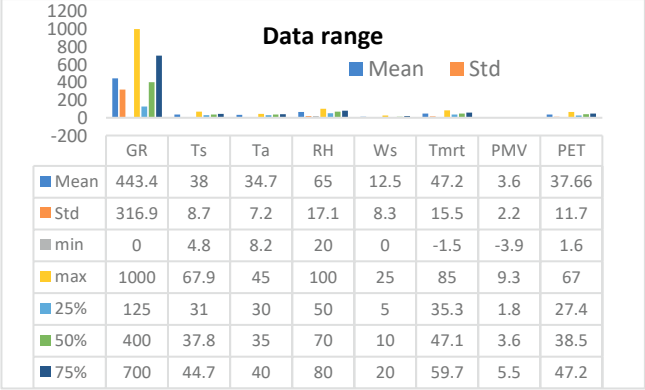

	GR	Ts	Ta	RH	Ws	Tmrt	PMV	PET
Mean	443.4	38	34.7	65	12.5	47.2	3.6	37.66
Std	316.9	8.7	7.2	17.1	8.3	15.5	2.2	11.7
min	0	4.8	8.2	20	0	-1.5	-3.9	1.6
max	1000	67.9	45	100	25	85	9.3	67
25%	125	31	30	50	5	35.3	1.8	27.4
50%	400	37.8	35	70	10	47.1	3.6	38.5
75%	700	44.7	40	80	20	59.7	5.5	47.2

Fig.4 Graphical presentation of data ranging

3.2 *Data Preparation*

This step is necessary to understand the dataset to avoid estimation problems. The correlated attributes of the data are discussed in the section above. This is the fastest way to see if the features correspond to the output.

3.3 Probability Density Function

To visualize the likelihood of an outcome in a given range, we estimated a Probability Density Function (PDF) from the available data. First, we observed the density of a random variable x with a simple histogram and identified the probability distribution p(x). The PDF is shown in Fig.5 (a) PET (b) PMV and (c) T_{mrt} discrete random variable and the probabilities $(P(X) = x)$ for all the possible values of x. The area below the curve indicates the interval in which the variable will fall and the total area of the interval is equal to the probability of occurrence of a single random variable.

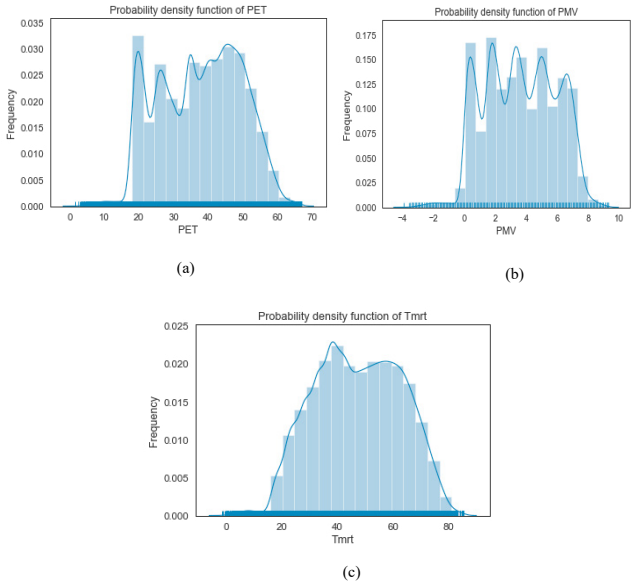

Fig.5 Probability distribution of (a) PET (b) PMV (c) T_{mrt}

3.4 Resampling

Resampling the dataset is necessary to generate confidence intervals, it helps to quantify the uncertainty, to gather data and best use in the predictive problem. After visualizing the dataset using PDF, the hourly data is resampled over 30 minutes, but it was observed that sum of the resampled dataset have similar structures.

3.5 Data scaling

Scaling and normalization is important where numeric values transforms and data points can have specific useful properties. The difference is that in scaling, the data range is changed while when normalizing, the shape of the data distribution is changed. Min: max scaling and normalization is the simplest method to resize the range of characteristics in [0, 1]. It is found by using eq. (1)

$$x' = \frac{x - min(x)}{max(x) - min(x)} \tag{1}$$

Sklearn library helps in making random partitions for both subsets for training data and for test data. X and Y arrays are divided into 4 more arrays, 70% of input and output data sets (73616, 5) (73616, 3) are trained for deep learning, 30% (31551, 5) (31551, 3) kept for testing phase to fully guarantee the randomness of each use of the data set.

3.6 The model architecture

For solving the vanishing gradient problem of a standard RNN, the GRU model uses update gate and reset gate. These are two vectors which decide what information should be passed and can trained to retain information from the past, without washing it out over time. It removes information which is irrelevant for the prediction. The model is based on governing eq. (2-5). The structure of the GRU is shown in Fig.6.

Where; x_t is an input vector, (T_{s}, T_{air}, GR, RH and W_{s}) h_t is an output vector (T_{mrt}, PMV, PET), h'_t is candidate activation vector, z_t is update gate vector, r_t is reset gate

vector, w_z and u_z are weight matrices it initializes to 0 or [-1, 1], b_n represents bias vectors with n ∈ r, h, σ_g is a sigmoid function:$S(x) = \frac{1}{1+e^{-x}}$ and $\phi_h$is original is a hyperbolic tangent: $\tanh_x = \frac{\sinh x}{\cosh x} = \frac{e^x - e^{-x}}{e^x + e^{-x}} = \frac{e^{2x}-1}{e^{2x}+1}$

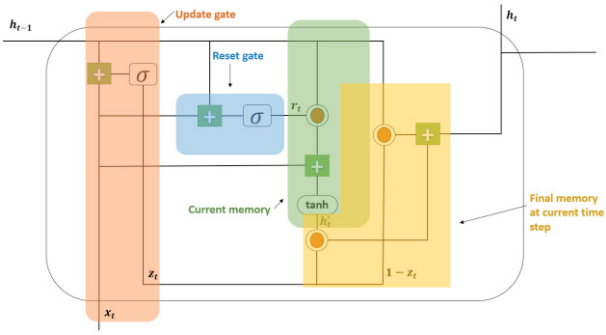

Fig.6 GRU Unit at time step t

We update the gate z for the time step t using eq. (2).

$$z_t = \sigma(w_z x_t + u_z h_{t-1} + b_z) \quad (2)$$

Vector x_t in matrix multiplied it with w_z and added with the multiplication of u_z and h_{t-1} (Note that h_{t-1}=0), then we have added results with the bias b, afterwards the sigmoid function was activated.

The reset gate is used, which helps to decide how much of the past information is needed to forget with the help of eq.(3)

$$r_t = \sigma(w_r x_t + u_r h_{t-1} + b_r) \quad (3)$$

This is the same as update gate, the difference comes from the weights and the usage of the gates, so these are two different vectors r_t and z_t. It is noticed that how exactly the gates affect the final output. It is started with the use of the reset gate and introduces a new memory content by using tanh which creates a new memory vector and store the relevant information from the past using eq. (4).

$$h'_t = \phi(w_h x_t + u_h(r_t \odot h_{t-1}) + b_h) \quad (4)$$

In the last step, the network calculates the current hidden state output vector h_t which holds information for the current unit and passes it down to the network. In order to do this, the update gate is required. It determines what to collect from the current memory content h'_t and what from the previous steps h_{t-1}. This is the final output calculated by using eq. (5).

$$h_t = (1 - z_t) \odot h_{t-1} + z_t \odot h'_t \quad (5)$$

3.7 Model convergence

The mean Square Error (MSE) loss function and the efficient Adam version of stochastic gradient descent is used to measure the accuracy and optimize the deep learning model. Adam optimization is a stochastic gradient descent method that is based on adaptive estimation of first and second order moments. It is the best among the adaptive optimizers with perfect adaptive learning rate. MSE is calculated by eq. (6). where n is the total amount of the dataset, Yi is the real observed $\hat{Y}_i$ is the estimated data.

$$\text{MSE} = \frac{1}{n}\sum_{i=1}^{n}\left(Y_i - \hat{Y}_i\right)^2 \quad (6)$$

$$RMSE = \sqrt{MSE}$$

The GRU network is implemented using the tensor flow deep learning package. Hereby, we provide a detailed description of our GRU based models as follows:

- The first visible input layer consists of 128 GRU cells, and the dropout rate is 0.5 with the relu activation function.
- Second hidden dense layer consists of 256 neurons with 3 outputs where the dropout rate is 0.25 and linear activation function sets for the last layer.
- Finally, the Adam optimization algorithm is used for network training. We set the patience of the training process over 40 epochs with a batch size of 256, can be seen in Fig.7.
- 70% of the data was used for learning and 30% of data in the dataset was employed as test data which is later used for the validation. An accuracy score of 99.36% is obtained with MSE= 0.0002.

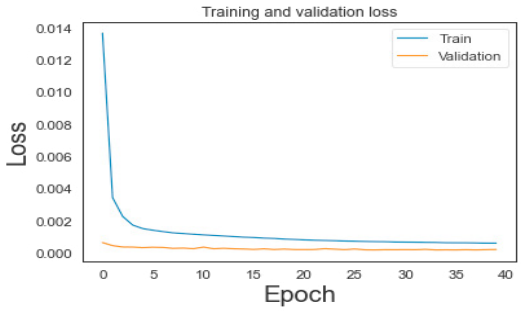

Fig.7 Graph of iteraction performed for training and validation

3.8 Model implementation

Based on the systems approach of this model, GR, RH, $,T_{air}$, $,W_s$ and $,T_s$ forms the input vector x_t, where x_t is represented as follows: [x_{t1} : GR; x_{t2} : $,T_s$; x_{t3} : $,T_{air}$; x_{t4} : RH; x_{t5} : $,W_s$]

Each row of the input matrix x_t is taken into the GRU unit and the obtained output (h_t) vectors are represented as follows: $[h_{t1} : T_{mrt}$; h_{t2} : PMV; h_{t3} : PET] respectively. Eq. (7-9) are used for predictions derived from governing eq. (2-5) of GRU model.

$$\begin{pmatrix} z_t \\ r_t \end{pmatrix} = \begin{pmatrix} \sigma \\ \sigma \end{pmatrix} \cdot \begin{bmatrix} w_z & u_z \\ w_r & u_r \end{bmatrix} \times \begin{pmatrix} x_t \\ h_{t-1} \end{pmatrix} + \begin{pmatrix} b_z \\ b_r \end{pmatrix} \quad (7)$$

$$h'_t = tanh_x \, [w_h \;\; u_h] \times \begin{pmatrix} x_t \\ r_t \odot h_{t-1} \end{pmatrix} + b_h \quad (8a)$$

$$h'_t = \left(\frac{e^{2x}-1}{e^{2x}+1}\right) . \, [w_h \;\; u_h] \times \begin{pmatrix} x_t \\ r_t \odot h_{t-1} \end{pmatrix} + b_h \quad (8b)$$

$$h_t = z_t \odot h'_t + (1 - z_t) \odot h_{t-1} \quad (9)$$

h_t is initialized from 0 so, h_{t-1} = 0, but at t=1, h_t changes and the weight matrices (w, u) of the input and output data of the previous cells updated by using eq. (10) [where α is

adjusting parameter which is >0] and error_t = error at time step t and learning rate controls the model in response to the estimated error each time to update the model weights.

$$W_{t+1} = W_t + error_t * \text{learning rate} * \alpha \quad (10)$$

3.9 Validation

The performance of the developed deep learning models was validated using the test data. This process was independent of the learning process of the algorithm. Validation process repeated twice. First, the input variables of 100 test samples from the test dataset. The resulting output (PET) of the model is plotted with the actual output of the dataset can be seen in Fig.8. To check the reliability of the model, another dataset with realistic summer measurements is used and plotted 300 examples (see Fig.9). We notice that the model responds efficiently and reliable results are obtained which are compared to the reference software.

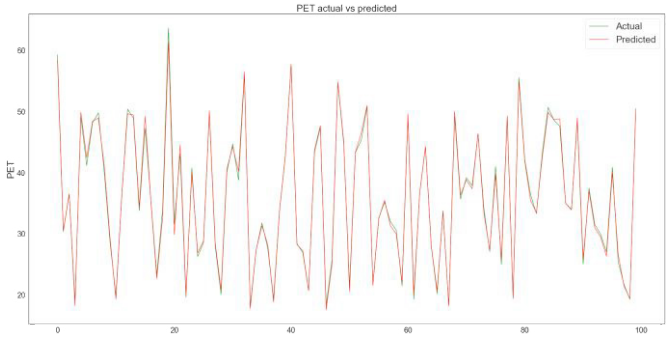

Fig.8 Validation of model outputs testing phase 1 for PET.

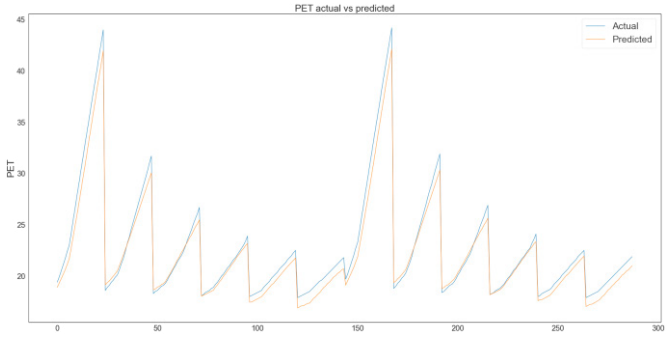

Fig.9 Validation of model outputs testing phase 2 for PET.

4. WEB BASED SIMULATION TOOL

After validation of the model, the open-source web framework based on Python, "Django" is used to develop the graphical user interface (GUI) for the evaluation of HS. This interface provides the platform for users to choose their thermal comfort scale based on their current feeling and considering the obtained assessment results plan outdoor activities. The interface also provides a platform where the users can compare their current comfort level with the given index results, which can help them compare their results and choose the index that matches with the situation. For example, it is shown in Fig.10d that PET and PMV results indicate the different comfort zones which may needs the user's assessment. The functions and use of the GUI are as follows:

- Home page (Fig.10a): It gives general information on thermal stress.
- Parameters (Fig.10b): Here users can either set the thermal comfort scale for PET according to their thermal perception or choose the standard default parameters and save them. Users can do the same for PMV and T_{mrt}.
- Predictions (Fig.10c): The input variables are necessary for the prediction.
- History (Fig.10d): It records entries and results calculated by random users.

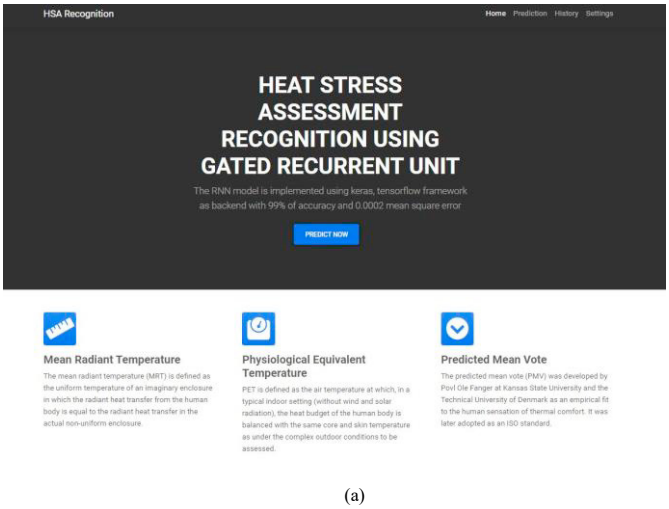

(a)

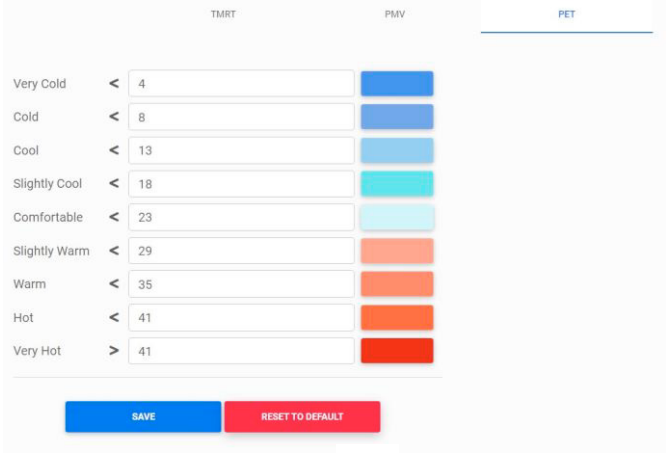

(b)

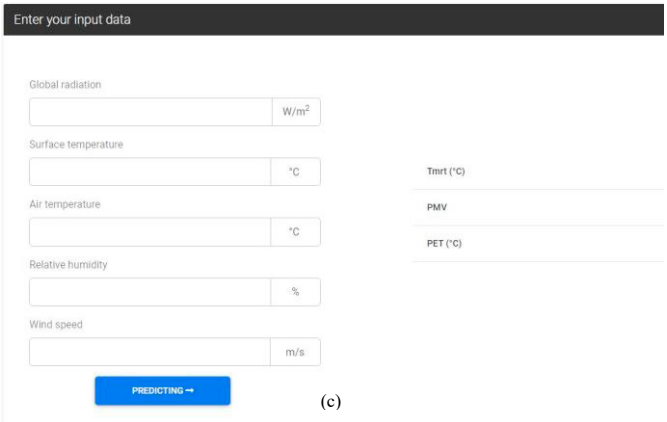

(c)

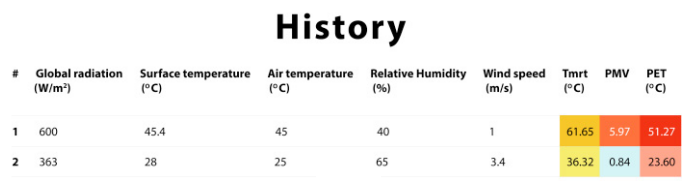

(d)

Fig.10 Pictorial View of GUI

5. CONCLUSION

In this study, system dynamic approach and GRU network is used as a powerful method to predict HS. The variables which strongly effects the system are analyzed and extracted as input variables (T_{air}, T_s, GR, RH, W_s). The GRU network is modeled, after using the grid search to find the optimal hyper-parameters and estimates the outputs (T_{mrt}, PET, PMV). For the given dataset, the proposed GRU training algorithm was 99.36% accurate. The model was coupled with GUI for individual HSA. This study concludes that system approach helps to assess HS even in the complex environment and address the nonlinear interactions of the variables. Also, a user can use this interface for their own comfort definition which will give the platform to analyze the different thermal comfort scale chosen by users. There are still some limitations in this study that requires further research. An optimization and extension in the model may be future work. It will be coupled with the cooling effect of urban greenery which may influence the estimation of HS.

ACKNOWLEDGEMENT

This paper has been produced within the COOL-TOWNS project which receives funding from the Interreg 2 Seas programme 2014-2020 co-funded by the European Regional Development Fund under subsidy contract N° 2S05-040.

REFERENCES

AKBARI, H., ROSENFELD, A. H. & TAHA, H. 1990. Summer heat islands, urban trees, and white surfaces.

ARNDS, D., BÖHNER, J. & BECHTEL, B. 2017. Spatio-temporal variance and meteorological drivers of the urban heat island in a European city. Theoretical and applied climatology, 128, 43-61.

CHO, K., VAN MERRIËNBOER, B., GULCEHRE, C., BAHDANAU, D., BOUGARES, F., SCHWENK, H. & BENGIO, Y. 2014. Learning phrase representations using RNN encoder-decoder for statistical machine translation. arXiv preprint arXiv:1406.1078.

FARHAN, A. A., PATTIPATI, K., WANG, B. & LUH, P. Predicting individual thermal comfort using machine learning algorithms. 2015 IEEE International Conference on Automation Science and Engineering (CASE), 2015. IEEE, 708-713.

FISCHER, E. M. & SCHÄR, C. 2010. Consistent geographical patterns of changes in high-impact European heatwaves. Nature geoscience, 3, 398-403.

GHAFFARIANHOSEINI, A., BERARDI, U., GHAFFARIANHOSEINI, A. & AL-OBAIDI, K. 2019. Analyzing the thermal comfort conditions of outdoor spaces in a university campus in Kuala Lumpur, Malaysia. Science of the total environment, 666, 1327-1345.

GRIMMOND, S. U. 2007. Urbanization and global environmental change: local effects of urban warming. Geographical Journal, 173, 83-88.

HEWAGE, P., TROVATI, M., PEREIRA, E. & BEHERA, A. 2021. Deep learning-based effective fine-grained weather forecasting model. Pattern Analysis and Applications, 24, 343-366.

HOFFMANN, P. 2012. Quantifying the influence of climate change on the urban heat island of Hamburg using different downscaling methods. Staats-und Universitätsbibliothek Hamburg Carl von Ossietzky.

HOFFMANN, P. & SCHLÜNZEN, K. H. 2013 b. Weather pattern classification to represent the urban heat island in present and future climate. Journal of Applied Meteorology and Climatology, 52, 2699-2714.

IVAJNŠIČ, D. & ŽIBERNA, I. 2019. The effect of weather patterns on winter small city urban heat islands. Meteorological Applications, 26, 195-203.

KALNAY, E. & CAI, M. 2003. Impact of urbanization and land-use change on climate. Nature, 423, 528-531.

KICOVIC, D., VUCKOVIC, D., MARKOVIC, D. & JOVIC, S. 2019. Assessment of visitors' thermal comfort based on physiologically equivalent temperature in open urban areas. Urban Climate, 28, 100466.

LUBER, G. & MCGEEHIN, M. 2008. Climate change and extreme heat events. American journal of preventive medicine, 35, 429-435.

MATZARAKIS, A., RUTZ, F. & MAYER, H. 2007 b. Modelling radiation fluxes in simple and complex environments—application of the RayMan model. International journal of biometeorology, 51, 323-334.

MATZARAKIS, A., RUTZ, F. & MAYER, H. 2010. Modelling radiation fluxes in simple and complex environments: basics of the RayMan model. International journal of biometeorology, 54, 131-139.

MCDONALD, R. I., GREEN, P., BALK, D., FEKETE, B. M., REVENGA, C., TODD, M. & MONTGOMERY, M. 2011. Urban growth, climate change, and freshwater availability. Proceedings of the National Academy of Sciences, 108, 6312-6317.

MIRZAEI, P. A. 2015. Recent challenges in modeling of urban heat island. Sustainable cities and society, 19, 200-206.

POUMADERE, M., MAYS, C., LE MER, S. & BLONG, R. 2005. The 2003 heat wave in France: dangerous climate change here and now. Risk Analysis: an International Journal, 25, 1483-1494.

TSOKA, S., TSIKALOUDAKI, A. & THEODOSIOU, T. 2018. Analyzing the ENVI-met microclimate model's performance and assessing cool materials and urban vegetation applications–A review. Sustainable cities and society, 43, 55-76.